# Neurotrophin-3 Prevents the Proximal Accumulation of Neurofilament Proteins in Sensory Neurons of Streptozocin-Induced Diabetic Rats

**Nicola M. Sayers,[1] Lisa J. Beswick,[1] Alicia Middlemas,[1] Nigel A. Calcutt,[2] Andrew P. Mizisin,[2] David R. Tomlinson,[1] and Paul Fernyhough[1]**

**The relation between neurofilament expression and/or phosphorylation in the proximal versus distal components of the sensory peripheral neuraxis was studied and related to disorders in structure and function of the distal axon of streptozocin (STZ)-induced diabetic rats studied for 14 weeks. The ability of neurotrophin-3 (NT-3) to prevent abnormalities in neurofilament biology was also investigated. Compared with age-matched controls, neurofilament heavy (NF-H) (3.3-fold) and neurofilament medium (NF-M) (2.5-fold), but not neurofilament light (NF-L), subunits accumulated in the proximal axon of sensory neurons of the lumbar dorsal root ganglia (DRG) in untreated diabetic rats. Neurofilament accumulation was prevented by NT-3. Small- and large-diameter sensory neurons exhibited elevated levels of NF-H protein accumulation and phosphorylation in the DRG of untreated diabetic rats, levels that were ameliorated by NT-3. The sural nerve of untreated diabetic rats showed a 50% decrease in the levels of NF-H and NF-M, but not NF-L, subunits; NT-3 only partially normalized the defect in NF-M expression. These observations were associated with significant lowering of motor and sensory nerve conduction velocity but no alteration in the mean axonal diameter of myelinated axons in the sural nerve in untreated diabetic rats. It is proposed that the accumulation of NF-H and NF-M subunits in the proximal axon is an etiologic factor in the distal axon degeneration observed in diabetes. *Diabetes* 52:2372–2380, 2003**

As the major constituents of the axonal cylinder, neurofilaments are heteropolymers comprised of protein units with a molecular mass of 200 kDa (neurofilament heavy subunits [NF-H]), 150 kDa (neurofilament medium subunits [NF-M]), and 70 kDa (neurofilament light subunits [NF-L]). In the streptozocin (STZ) and BB rodent models of type 1 diabetes, structural abnormalities in peripheral nerve include decreased axonal caliber or axonal dwindling (1–3). Studies in type 1 diabetic rats show reduced expression of neurofilaments in sensory neurons (1,4,5), reduced axonal transport of neurofilament in sensory axons (6), loss of neurofilament in distal nerve (1–3,7), and abnormal neurofilament phosphorylation in the dorsal root ganglia (DRG), spinal cord, and sciatic nerve (8–11). Aberrant phosphorylation of NF-H and NF-M subunits in DRG of STZ- and BB-diabetic rats is associated with activation of c-jun $NH_2$-terminal kinase (JNK) (10). The stress-activated protein kinases (SAPKs: extracellular signal–regulated kinase [ERK], JNK, and p38) are well-characterized proteins that phosphorylate neurofilaments and are activated by hyperglycemia and oxidative stress in cultured sensory neurons (11–13).

Nerve crush–induced loss of neurofilament expression in the small-to-medium subpopulation of neurons in the DRG is ameliorated by nerve growth factor treatment (14,15). Sequestration of the high-affinity receptor for neurotrophin-3 (NT-3) results in motor and sensory nerve conduction velocity (NCV) deficits similar to those that develop after nerve transection (16). Exogenous NT-3 provided after physical nerve injury can prevent and reverse a range of injury-evoked responses (16–18) and also enhance subsequent regeneration (19). Systemic NT-3 treatment has also been shown to prevent toxin-induced peripheral neuropathies (20,21). Demonstration of altered expression of NT-3 and its receptors in DRG, nerve, and muscle in STZ-induced diabetic animals suggests that loss of NT-3-dependent neurotrophic support may contribute to the pathogenesis of diabetic neuropathy (22–24). In the galactose-fed rat model of diabetes and in the STZ-induced diabetic rat, NT-3 treatment prevents axonal atrophy of sensory nerves and slowing of sensory nerve conduction velocity (SNCV) in the sciatic nerve (3,25).

The objective of this study was to determine the relation between neurofilament expression and phosphorylation in the proximal versus distal components of the peripheral sensory neuraxis and to relate any findings to disorders in the structure and function of the distal axon in STZ-induced diabetic rats. The effect of exogenous NT-3 treatment on the abnormalities in neurofilament biology in STZ-induced diabetic rats was also investigated. Axonal caliber and neurofilament number in the sensory sural nerve were measured as an index of nerve structure, and

From the [1]School of Biological Sciences, University of Manchester, Manchester, U.K.; and the [2]Department of Pathology, University of California at San Diego, La Jolla, California.

Address correspondence and reprint requests to Dr. Paul Fernyhough, 1.124 Stopford Bldg., School of Biological Sciences, University of Manchester, Oxford Road, Manchester M13 9PT, U.K. E-mail: paul.fernyhough@man.ac.uk.

Received for publication 10 February 2003 and accepted in revised form 5 June 2003.

DRG, dorsal root ganglia; JNK, c-Jun $NH_2$-terminal kinase; ERK, extracellular signal–regulated kinase; FITC, fluorescein isothiocyanate; MNCV, motor nerve conduction velocity; NCV, nerve conduction velocity; NF-H, neurofilament heavy subunit; NF-L, neurofilament light subunit; NF-M, neurofilament medium subunit; NT-3, neurotrophin-3; SAPK, stress-activated protein kinase; SNCV, sensory nerve conduction velocity; STZ, streptozocin.

the motor nerve conduction velocity (MNCV) and SNCV in the sciatic nerve were used as indexes of peripheral nerve function that may be influenced by axonal caliber.

## RESEARCH DESIGN AND METHODS

**Induction of diabetes and NT-3 treatment.** Male Wistar rats (300 g) were made diabetic by a single injection of STZ (55 mg/kg i.p.; Sigma) and maintained in parallel with age-matched control animals. Tail blood glucose was assayed 3 days after injection using glucose test strips (BM-Accutest; Roche Diagnostics, Basel, Switzerland) to confirm diabetes. All diabetic animals had blood glucose values >30 mmol/l. Rats were maintained for 14 weeks with free access to water and laboratory diet. One group of diabetic rats received injections (5 mg/kg s.c.) of human recombinant NT-3 (a gift from Regeneron Pharmaceuticals, Tarrytown, NY) three times weekly for the final 10 weeks of the 14-week diabetes study. Final body weights were as follows: age-matched controls, 629 ± 18.5; STZ-induced diabetic rats, 347 ± 16.0; and STZ-diabetic + NT-3 rats, 389 ± 19.0 (means ± SE; $n = 6–8$; $P < 0.001$ for control vs. other groups by one-way ANOVA). Immediately after the death of the animals, a blood sample was taken and the plasma glucose concentration was determined using the GOD-PERID test kit (Boehringer Mannheim, Germany).

**Motor and sensory NCV measurement.** NCVs were measured by subtracting the distal latencies for M waves (MNCV) and H reflexes (SNCV) elicited by stimulation at the sciatic notch and Achilles tendon. The principles and practicalities of these methods have been described in detail elsewhere (26). In the present investigation, the measurements were performed on rats under isofluorane anesthesia. The core body temperature was monitored by a rectal probe and maintained at ~37°C. The temperature adjacent to the sciatic nerve was monitored by a microthermocouple connected to an electronic thermometer (Comark Electronics, Rustington, U.K.). NCVs were assessed in all animals during the final week before being culled. The procedure was approved as part of the Home Office Project License awarded to D.R.T.

**Morphometric analysis of axonal caliber.** Sural nerves were processed for light microscopic examination by immersion fixation in 2.5% phosphate-buffered glutaraldehyde (37°C) for ~3 h. The nerves were then fixed overnight in 2.5% phosphate-buffered glutaraldehyde at 4°C. Tissue was postfixed in 1% aqueous osmium tetroxide for 3–4 h before being dehydrated using a series of graded alcohols and propylene oxide. After being infiltrated with a 1:1 mixture of propylene oxide and araldite for 4 h, nerves were placed in 100% araldite overnight before being embedded in fresh araldite resin. Thick sections (1 μm) were cut with glass knives and stained with *p*-phenylenediamine before they were studied with a light microscope. Computer-assisted analyses of axonal size-frequency distributions of myelinated fibers were performed on nerves, as described earlier (25). Single sections of the sural nerve from each animal were sampled. A video image was obtained for each nerve with an Olympus BH-2 light microscope and Cohu 5000 series television camera interfaced with a Macintosh Quadra 850AV computer running the National Institutes of Health's Image 1.55 software. Myelinated fibers with axons >1 μm in diameter were individually identified and selected before being sorted with an automated process into bins based on axonal diameter. In each case, systematic sampling of nonoverlapping fields resulted in sampling 50–80% of the total myelinated fibers in each nerve. Neurofilament density and number in the sural nerve were calculated as previously described (27). Thin sections (60 nm) were cut with a diamond knife and stained with uranyl acetate and bismuth subnitrate before being viewed with a Zeiss 10 electron microscope operated at 80 keV. Electron micrographs of cross-sections of axons from 3–15 myelinated fibers per nerve were taken at a magnification of ×10,000 and printed at a final magnification of ×58,000. An acetate with templates of evenly spaced circles was put over each print, and the number of neurofilaments within each circle was counted to determine density. The total area of each axon was then digitized and multiplied by neurofilament density to determine total neurofilament number.

**Quantification of neurofilament levels by Western blotting.** The L4–L5 DRG, proximal nerve (5 mm of spinal nerve directly adjacent and distal to the DRG, containing mainly sensory and motor fibers), and sural nerve (mainly sensory, but with some autonomic content) were isolated from control, diabetic, and NT-3–treated animals and immediately frozen on dry ice. The tissues were homogenized in 450–500 μl homogenization buffer (50 mmol/l Tris-HCl [pH7.4], 1% NP-40, 0.25% sodium deoxycholate; 150 mmol/l NaCl; 1 mmol/l EGTA; 1 mmol/l phenylmethylsulfonyl fluoride; 1 μmol/ml aprotinin; leupeptin; pepstatin; 1 mmol/l $Na_3VO_4$; and 1 mmol/l NaF). Protein concentrations were determined using a bromophenol-blue–based protein assay. For SDS-PAGE, 5 μg of protein were loaded into each well and then transferred to nitrocellulose. The nitrocellulose paper was rinsed with 0.5% Tween-20 in PBS for 10 min. After being blocked with 5% nonfat dry milk in PBS for 1 h at room temperature, the blotted nitrocellulose was incubated with diluted primary antibodies against total NF-H (COOH-terminal antibody from Chemicon; diluted 1:10,000), total NF-M (RM044 from Zymed; diluted 1:10,000), phosphorylated NF-H and NF-M (SMI-31 from Sternberger; diluted 1:10,000), total NF-L (Chemicon; diluted 1:1,000), total JNK (Santa Cruz Biotechnology, Santa Cruz, CA; code FL; diluted 1:1,000), phosphorylated JNK (Santa Cruz; code G-7; diluted 1:200; phosphorylated on Thr-183 and Tyr-185), total p38 (New England Biolabs, Beverley, MA; code 9212; diluted 1:1,000), phosphorylated p38 (Biosource International, Camarillo, CA; code 44–684; diluted 1:2000; phosphorylated on Thr-180 and Tyr-182), and phosphorylated ERK (New England Biolabs; code 9101; diluted 1:4,000; phosphorylated on Thr-202 and Tyr-204). Incubations were followed by treatment with secondary antibody (horseradish peroxidase–conjugated anti-mouse/rabbit secondary antibody [Cell Signaling, 1:2,500]) at room temperature for 1.5 h. Enhanced chemiluminescence (LumiGlu; Cell Signaling) was used to detect the signal from the blot. The bands in the X-ray film were scanned and quantitated using the Molecular Analysis image analysis software package (Version 1.5, Biorad).

**Immunohistochemistry for neurofilament in DRG.** Lumbar DRGs from control, diabetic, and NT-3 treated animals ($n = 3$) were fixed in situ, as previously described (10). These animals were used at the 12-week time point of the 14-week study. Animals were anesthetized by injection of sagatal (1 ml/kg i.p.). Blood vessels were perfused with ice-cold saline via the left ventricle with a peristaltic pump (Watson Marlow, Falmouth, U.K.) at a rate of 25 ml/min for 8 min to replace blood, followed by perfusion with ice-cold 4% paraformaldehyde (in 0.1 mol/l phosphate buffer [pH 7.4]) for 15 min. L4–L5 DRG were dissected and postfixed in 4% paraformaldehyde for 4 h at 4°C. The fixed tissues were washed in PBS overnight at 4°C and soaked in 30% sucrose for 2 h at 4°C. The tissues were put in embedding medium and placed on dry ice until frozen. Sections (11 μm) were cut and placed on polylysine-coated slides. Nonspecific binding was blocked by incubation with 10% donkey serum for 2 h at room temperature. The slides were then washed with PBS three times. Fixed tissues were incubated with the primary antibodies described above overnight at 4°C followed by fluorescein isothiocyanate (FITC)-conjugated secondary antibody (1:200) for 1.5 h at room temperature. Fluorescence was examined using a Leica DMR fluorescence microscope with an FITC filter, and images were collected with a Hamamatsu C4742–95 digital camera.

For quantification of the SMI-31 signal intensity in DRG, the serial sections were individually analyzed using MetaFluor/MetaMorph software (Universal Imaging, Westchester, PA). Single neuron perikarya were identified and the signal for fluorescence intensity collected. At least three DRG sections for each animal were analyzed, and three animals were studied for each treatment. Every neuronal perikaryon in every section was analyzed; the cell numbers assessed for each treatment group ranged from 35 to 100.

**Statistical analysis.** Where appropriate, data were subjected to one-way ANOVA using the statistical package SPSS/PC+ (SPSS, Chicago, IL). Where the $F$ ratio gave $P < 0.05$, comparisons between individual group means were made by Scheffe's multiple-range test at significance levels of $P = 0.05$. Where nonhomogeneity of variance was apparent, single comparisons were performed using Student's $t$ test at significance levels of $P < 0.01$.

## RESULTS

**NCV, axonal caliber, and neurofilament numbers in sural nerve.** The STZ-induced diabetic rats exhibited characteristic reduced body weight and increased plasma glucose levels (Table 1). NT-3 treatment had no effect on these parameters. MNCV and SNCV were both significantly lower in STZ-induced diabetic rats, and NT-3 treatment prevented the deficit in SNCV but not MNCV (Table 1). No qualitative differences were evident in axons of myelinated fibers from the sural nerve (Fig. 1), suggesting that STZ-induced diabetes and NT-3 treatment had no effect. Likewise, quantitative measures of axonal diameter and neurofilament density and number in myelinated axons of the sural nerve were not significantly altered in STZ-induced diabetic rats (Table 1), although there was a nonsignificant 27% reduction in the number of neurofilaments. NT-3 treatment raised axonal diameter in STZ-induced diabetic rats by ~9%, but this effect was not statistically significant ($P < 0.18$).

TABLE 1
Effect of diabetes and NT-3 treatment on plasma glucose, NCV, and axon morphometry

| | Plasma glucose (mmol/l) | MNCV (m/s) | SNCV (m/s) | Mean axonal diameter (μm) | Neurofilament density (#/μm$^2$) | Neurofilament number per axon |
|---|---|---|---|---|---|---|
| Control | 7.2 ± 0.42† | 53.9 ± 1.9* | 56.4 ± 1.4 | 4.47 ± 0.06 | 120 ± 17.3 | 2,118 ± 357 |
| STZ-induced diabetic | 32.6 ± 1.14 | 38.1 ± 2.3 | 44.6 ± 2.6‡ | 4.36 ± 0.26 | 123 ± 26.0 | 1,546 ± 226 |
| Diabetic + NT-3 | 33.1 ± 2.0 | 37.4 ± 1.5 | 56.4 ± 2.4 | 4.79 ± 0.16 | 112 ± 8.70 | 1,696 ± 202 |

Data are means ± SE ($n$ = 6–8; $n$ = 3 for morphometric nerve data). STZ-induced diabetic rats were maintained for 14 weeks and treated with NT-3 (5 mg/kg s.c.) for the final 10 weeks. Age-matched control animals were used. Sciatic nerve MNCV and SNCV (H reflex) was assessed in the final week. Mean axonal diameter of fibers >1 μm in axon diameter and associated morphometric analysis of neurofilaments were measured from sural nerve (3–15 axons/nerve). *$P < 0.001$ for control vs. other groups (one-way ANOVA); †$P < 0.001$ for control vs. other groups ($t$-test); ‡$P < 0.001$ for diabetic vs. other groups (one-way ANOVA).

**Effect of NT-3 on the diabetes-induced accumulation of NF-H and NF-M in proximal nerve.** Levels of total NF-H and NF-M proteins (detected using antibodies specific for phosphorylation independent epitopes) were raised by 3.3- and 2.5-fold, respectively, in proximal nerve (5-mm nerve segment adjacent and distal to DRG) of STZ-induced diabetic rats, and these accumulations were completely prevented by NT-3 treatment (Fig. 2). In comparison, NF-H and NF-M phosphorylation status (detected using antibody SMI-31) was reduced by 50 and 80%, respectively; NT-3 normalized this abnormality. There was no diabetes-induced alteration in NF-L protein levels (Table 2).

**NF-H, NF-M, and NF-L protein levels in sural nerve.** Levels of total and phosphorylated NF-H and NF-M were lowered by ~50% in sural nerve of STZ-induced diabetic rats (Fig. 3). NT-3 treatment did not significantly reverse this decline in neurofilament protein levels; however, there was an ~25% increase in total and phosphorylated NF-M. There was no change in NF-L protein levels (Table 2).

**Neurofilament protein levels and phosphorylation status in DRG.** In lumbar DRG, the levels of total NF-H were raised fourfold in STZ-induced diabetic rats, with NT-3 significantly ameliorating this effect (Fig. 4). Immunohistochemical analysis of DRG revealed elevated expression of total NF-H in individual sensory neurons that was prevented by NT-3 (Fig. 5*D*–*F*; indicated by arrows). The Western blot analysis showed that the phosphorylation status of NF-H was also raised in diabetes by ~30% ($P < 0.05$), although NT-3 had no effect on this parameter. Total levels of NF-M were reduced by ~30% in STZ-induced diabetic rats, and NT-3 treatment had no effect (Fig. 4). Phosphorylation levels of NF-M were raised by 20–30% in STZ-induced diabetic rats, with the highest levels seen in the NT-3-treated animals. In contrast to the Western blotting data, the immunohistochemical analysis, using the SMI-31 antibody that detects phosphorylated epitopes on NF-H and/or NF-M, showed that phosphorylation of NF-H and NF-M was clearly upregulated in sensory neuron cell bodies of STZ-induced diabetic animals (Fig. 5*A*–*C*; arrows show sensory neurons in DRG of STZ-induced diabetic animals with particularly high signal intensity). Quantification of the fluorescence intensity of the SMI-31 signal showed that large (>30 μm in diameter) and small (<30 μm) sensory neurons underwent an elevation in NF-H/NF-M phosphorylation in DRG of STZ-induced diabetic rats (Fig. 6). The effect was greatest in large neurons, and NT-3 significantly prevented this increase in phosphorylation (Fig. 6). Again, NF-L protein levels measured using Western blotting were not significantly affected by diabetes or NT-3 treatment (Table 2).

**Influence of STZ-diabetes and NT-3 treatment on activation of SAPKs in DRG.** The neurofilament protein kinases, ERK-1 and -2, JNK (46-kDa and 54- to 56-kDa isoforms), and p38 all exhibited elevated activation (1.5- to 3.5-fold increase over control) in DRG of STZ-induced diabetic animals (Fig. 7). NT-3 failed to significantly affect the activation status of any of these protein kinases.



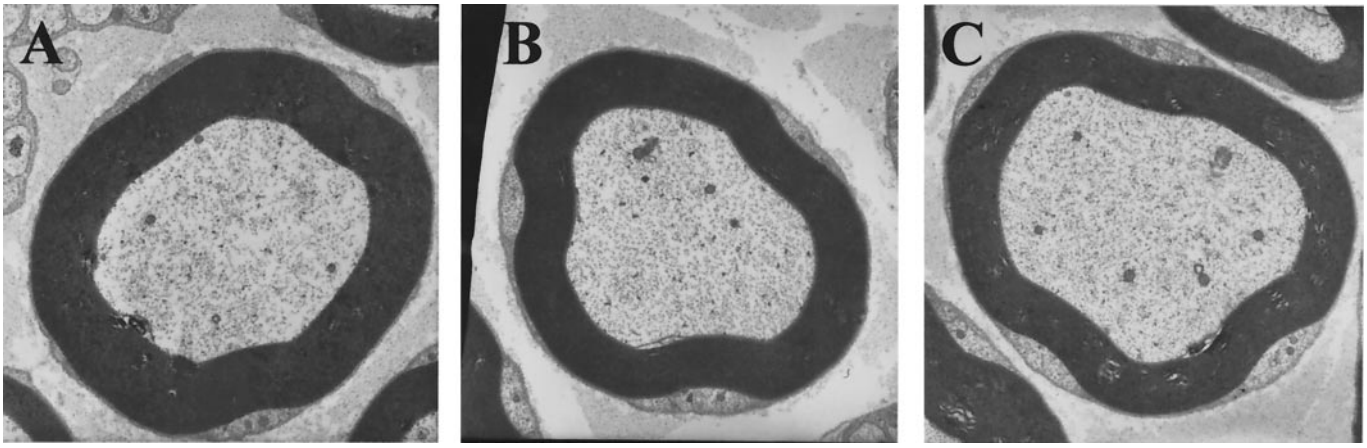


**FIG. 1. Representative myelinated fibers used for quantification of neurofilament density and number in the sural nerve. Axoplasm in internodal profiles from control (*A*), diabetic (*B*), and NT-3-treated diabetic (*C*) animals were not hydropic and appeared qualitatively similar. Original magnification ×10,000.**

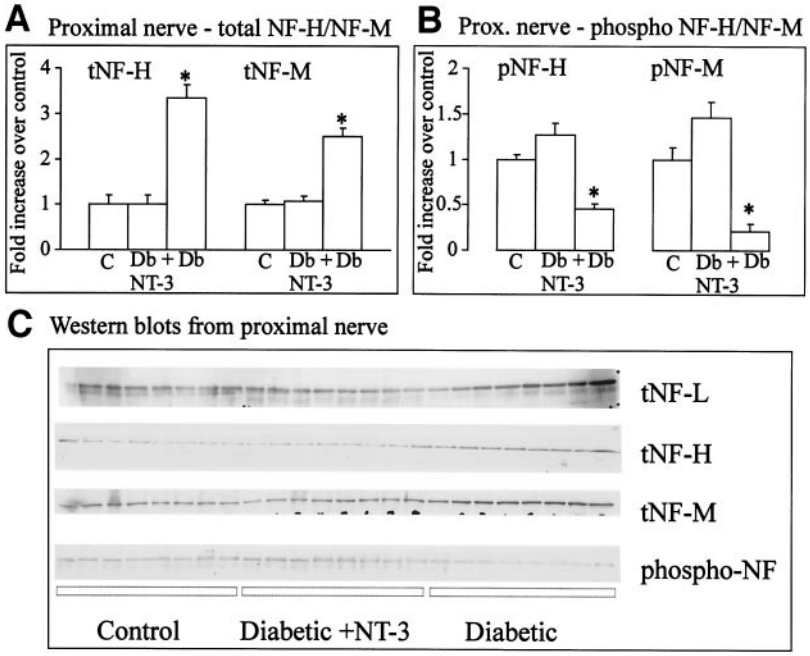


**FIG. 2. NT-3 prevents accumulation of NF-H and NF-M proteins in proximal nerve in STZ-induced diabetic rats. Proximal nerve (5 mm directly adjacent and distal to L4 and L5 DRG) was isolated from control, 14-week STZ-induced diabetic, and NT-3-treated animals and subjected to quantitative Western blotting. *A* and *B*: Data for total NF-H (tNF-H) and total NF-M (tNF-M) and phosphorylated NF-H (pNF-H) and phosphorylated NF-M (pNF-M). C, control; Db + NT-3, STZ-induced diabetic + NT-3; Db, STZ-induced diabetic. Data are normalized to control and are means ± SE ($n$ = 6–8). *C*: Western blot images. phospho-NF, phosphorylated NF. *$P$ < 0.05 for Db vs. other groups (one-way ANOVA).**

## DISCUSSION

The results of the present study showed that in proximal nerve and perikarya of sensory neurons in STZ-induced diabetic rats maintained for 14 weeks, there is an accumulation of NF-H and NF-M, but not NF-L, proteins. This proximal buildup coexisted with a 50% decrease of NF-H and NF-M, but not NF-L, in sural nerve. Treatment with NT-3 corrected the abnormalities in DRG and proximal nerve but only had a partial effect in restoring sural nerve neurofilament levels to normal.

**Reduced NCV and alterations in neurofilament expression were not associated with axonal atrophy.** Although sensory and motor NCV were reduced, the axon caliber in sural (Table 1) and peroneal nerve (i.e., motor axon; data not shown) was not significantly affected by diabetes. This observation is controversial in diabetic neuropathy, but these data confirm that early alterations in NCV are not associated with structural abnormalities in nerve in experimental diabetes. Therefore, relating the NCV change in STZ-induced diabetic rats to those observed in humans should be approached with caution. NT-3 treatment prevented the sensory NCV deficit but had no effect on motor NCV, a finding that conflicts with those of our previous study (3). This disparity may relate to differences in rate and extent of maturation of rats. The previous study was performed in the Mizisin/Calcutt laboratory using younger animals that may be more sensitive to NT-3 treatment with regard to NCV physiology. The current results showed that abnormalities in neurofilament biology in STZ-induced diabetic rats lag far behind the decrease in NCV, thereby supporting the view that

TABLE 2
Effect of STZ-diabetes and NT-3 treatment on total NF-L levels in the DRG and proximal and sural nerve

| | DRG | Proximal nerve | Sural nerve |
|---|---|---|---|
| Age-matched control | 1.0 ± 0.14 | 1.0 ± 0.01 | 1.0 ± 0.32 |
| STZ-induced diabetic | 0.78 ± 0.1 | 0.99 ± 0.01 | 0.92 ± 0.45 |
| Diabetic + NT-3 | 0.92 ± 0.07 | 0.98 ± 0.01 | 0.83 ± 0.23 |

Data are means ± SE ($n$ = 6–8). Western blots from DRG and proximal and sural nerves were performed and probed with antibody against all forms of NF-L. Data have been normalized to those of age-matched controls.

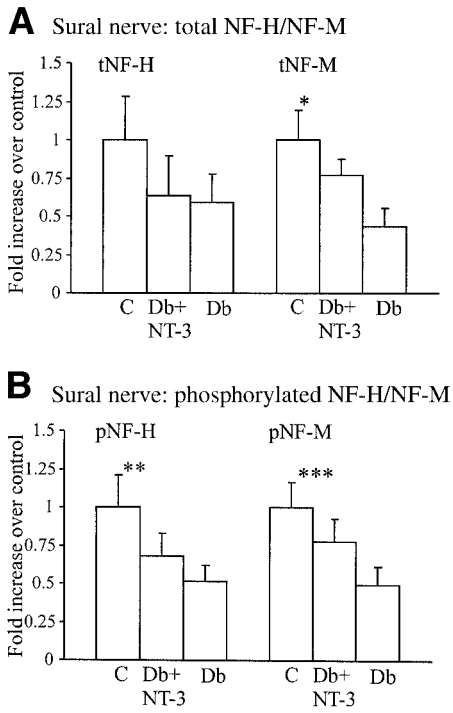


**FIG. 3. Levels of NF-H and NF-M proteins are decreased in sural nerve of STZ-induced diabetic rats. Sural nerve samples were subjected to quantitative Western blotting. *A*: Data for total NF-H (tNF-H) and total NF-M (tNF-M) in sural nerve. *B*: Data for phosphorylated NF-H (pNF-H) and phosphorylated NF-M (pNF-M) in sural nerve. Data are normalized to control and are means ± SE ($n$ = 5–7). C, control; Db + NT-3, STZ-induced diabetic + NT-3; Db, STZ-induced diabetic. *$P$ < 0.05 for control vs. diabetic (one-way ANOVA); **$P$ < 0.05 for control vs. other groups (one-way ANOVA); ***$P$ < 0.05 for control vs. diabetic ($t$ test).**

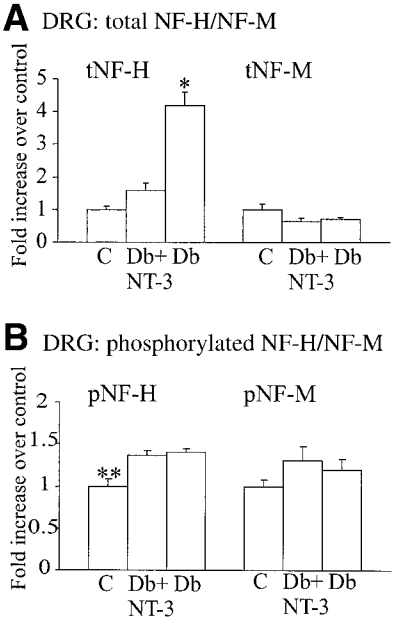


**FIG. 4. NF-H protein level, but not NF-M, rises in lumbar DRG in STZ-induced diabetic animals and is prevented by NT-3 treatment. L4 and L5 DRG were subjected to quantitative Western blotting. Shown are data for total NF-H (tNF-H) and total NF-M (tNF-M) (*A*) and phosphorylated NF-H (pNF-H) and phosphorylated NF-M (pNF-M) (*B*) in DRG. Data are normalized to control and are means ± SE ($n = 8$). C, control; Db + NT-3, STZ-induced diabetic + NT-3; Db, STZ-induced diabetic. *$P < 0.05$ for diabetic vs. other groups (one-way ANOVA); **$P < 0.05$ for control vs. other groups (one-way ANOVA).**

electrophysiological alterations in nerve function are not attributable to endoskeleton-based structural changes in the axon.

NF-H and NF-M protein levels were reduced by 50% in sural nerve (Fig. 3) but did not correlate with loss in axonal caliber, alterations in neurofilament density (Table 1), or changes in axon integrity. This indicates that nodal gaps were normal and that there was no hydropic axoplasm (Fig. 1). Although there was a 27% decrease in neurofilament number in sural nerve of STZ-induced diabetic rats, this was not statistically significant. These results match the control data and fall between the values for neurofilament numbers obtained by Scott et al. (1) at 2 and 6 months of STZ-induced diabetes. In our previous study at 3 months of STZ-induced diabetes, the mean axonal diameter of the largest myelinated fibers in sural nerve was significantly reduced by 7%, a reduction associated with reductions in NCV and loss of NF-H and NF-M protein. NT-3 treatment corrected the deficits in NCV and axonal caliber and partially normalized alterations in neurofilament phosphorylation but did not prevent the loss of NF-H and NF-M protein in sural nerve (3). These observations suggest that at 3 months of STZ-induced diabetes, the loss of NF-H and NF-M protein and the trend toward the reduction in neurofilament numbers (Table 1) in sural nerve are not critical determinants in the regulation of axonal caliber.

These findings confirm, in part, the results of neurofilament gene targeting studies in transgenic mice. Knockout of the NF-H gene or removal of the COOH-terminal of NF-H has no effect on axonal caliber in sciatic nerve (28–30); however, complete loss of NF-M expression does reduce axon caliber in sensory axons, possibly through impaired control of NF-L assembly (31,32). Studies in double-knockout mice for NF-H and NF-M show severe axonal atrophy associated with impaired expression and axonal transport of NF-L in sciatic nerve (32). The complete absence of NF-H and NF-M results in the failure of NF-L subunits to assemble, leading to loss of 10-nm filaments (32). Furthermore, the loss of NF-L expression via targeted disruption results in the failure of NF-H and NF-M to assemble, a scarcity of 10-nm filaments, and severe axonal atrophy (33). In the present study, NF-L protein levels were sustained at normal levels in the DRG and proximal and sural nerve of STZ-induced diabetic rats (Table 2). Our results suggest that more severe loss of NF-H and NF-M protein expression and delivery to the axon is required before an impact on NF-L assembly is produced and subsequent axonal atrophy develops. Therefore, if we had extended this study by 1–2 months, the axonal atrophy may have appeared and could have been associated with a significant loss in neurofilament number. With a longer duration of STZ-induced diabetes (≥6 months), axonal atrophy is more pronounced, is observed in both myelinated and unmyelinated fibers, and is associated with the loss of 10-nm filament numbers in axons (1,2).

**Mechanism of accumulation of NF-H and NF-M in proximal nerve and DRG.** The accumulation of NF-H within the perikarya of sensory neurons in the DRG was accompanied by a small but significant increase in phosphorylation (Figs. 4*B*, 5*A–C*, and 6). This accumulation of NF-H proteins was not associated with any ultrastructural changes within the DRG; for example, perikaryal sizes were normally distributed and intraganglionic nerve fibers appeared unaffected (data not shown). Although phosphorylation-dependent retardation of axonal transport of NF-H is feasible (34,35), the COOH-terminal of NF-H, which is the main site of phosphorylation, is not critical for the regulation of axonal transport of cargoes (30). Furthermore, the accumulation of NF-H and NF-M in the proximal nerve of diabetic rats was associated with a 50–80% decrease in the level of phosphorylation (Fig. 2*B*). Hypophosphorylated NF-H and NF-M undergo more rapid axonal transport (34) and, importantly, more readily form stable complexes with kinesin (36). Furthermore, postnatal deletion of KIF-5A, a neuronal-specific kinesin, results in impaired axonal transport of neurofilament and induces accumulation in sensory neuron cell bodies and axonal shrinkage in dorsal root (37). The energy dependency of kinesin-associated cargo motility, coupled with the mitochondrial dysfunction (38,39) and energy deficiency (40) characteristic of diabetes, may therefore explain impaired protein transport observed in STZ-induced diabetes (6).

**Mechanism of NT-3–dependent prevention of neurofilament accumulation.** NT-3 treatment normalized aberrant NF-H phosphorylation in small- and large-sized sensory neurons (Figs. 5 and 6). At a dosage of 5.0 mg/kg, NT-3 may influence neurofilament biology in a wide range of sensory neuron phenotypes via binding to trkC, trkA, and/or $p75^{NTR}$ (41,42). Although NT-3 reduced NF-H phosphorylation in perikarya of DRG (Figs. 5*A–C* and 6), it raised NF-H and NF-M phosphorylation in the proximal nerve (Fig. 2). We believe all these results are independent of direct modulation of neurofilament function by phos-

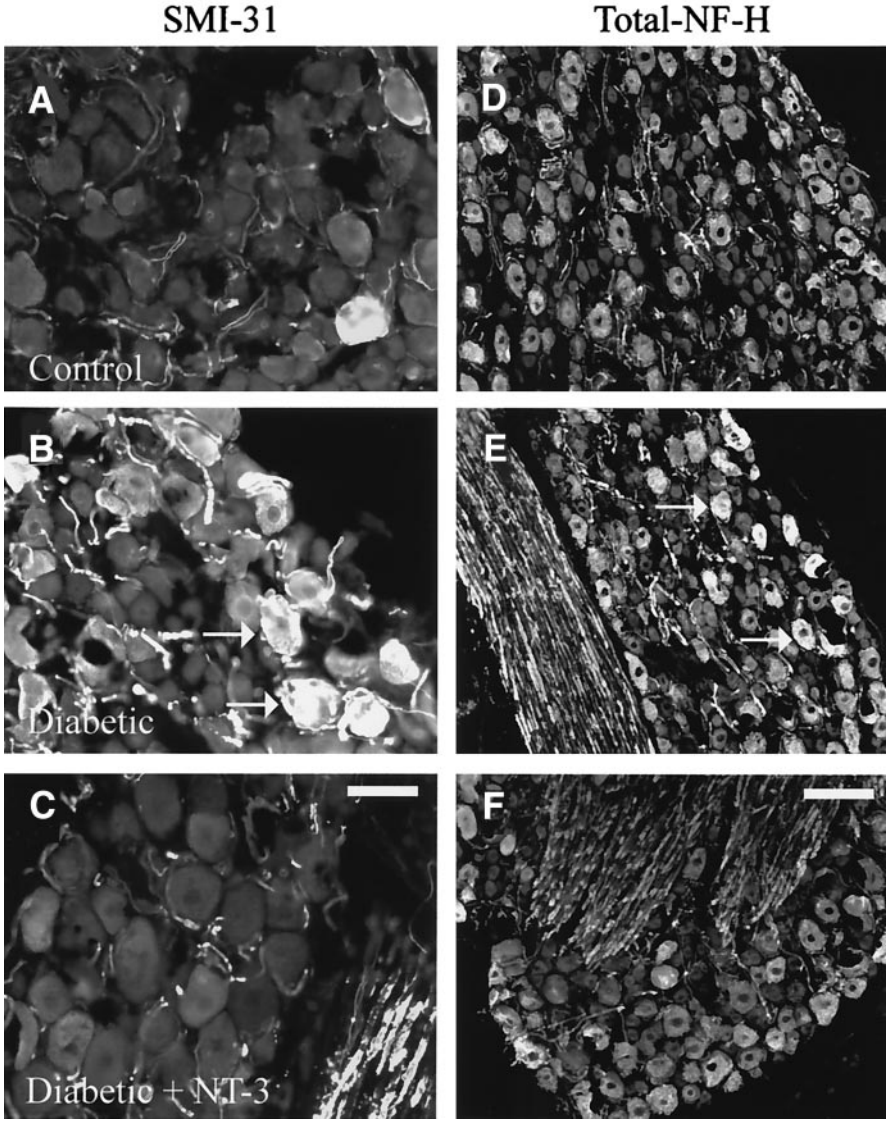


**FIG. 5. Immunohistochemical analysis of DRG demonstrates increased NF-H phosphorylation and levels in neuronal soma in STZ-induced diabetic rat model and prevention by NT-3. Sections of L4 and L5 DRG were analyzed using fluorescence immunohistochemistry with antibodies against phosphorylated NF-H/NF-M (SMI-31) or against total NF-H. Representative DRG sections in control (*A*), STZ-induced diabetic (*B*), and diabetic + NT-3 (*C*) were all probed using antibody to phosphorylated NF-H/NF-M (SMI-31). Total NF-H levels were assessed in control (*D*), STZ-induced diabetic (*E*), and diabetic + NT-3 (*F*). Arrows highlight neurons expressing high levels of phosphorylated or total NF-H/NF-M. Scale bars are 50 (*A–C*) and 100 μm (*D–F*).**

phorylation and instead are indicative of NT-3–dependent translocation of NF-H and NF-M away from the site of accumulation in the proximal axon. The increased activation of SAPKs (neurofilament kinases) in DRG of STZ-diabetic rats may have been expected to contribute significantly to the raised NF-H phosphorylation observed (Figs. 4*B* and 7). However, NT-3 failed to alter the phosphorylation status of these neurofilament kinases and, hence, involvement of these proteins in the etiology of neurofilament accumulation is unlikely. In fact, in the proximal axon, the SAPKs were activated two- to threefold (43) in association with a decrease in phosphorylation of NF-H and NF-M (Fig. 2*B*). NT-3 may act at two major loci to normalize neurofilament biology. NT-3 could augment neurofilament synthesis at the transcriptional and/or post-transcriptional levels; in fact, we have unpublished data showing that NT-3 can reverse the STZ diabetes-induced decrease in NFH and NFM mRNA levels. However, we favor a role for NT-3 in optimizing energy reserves within the sensory axon, possibly via direct modulation of mitochondrial function. Preliminary data demonstrating that NT-3 increases the mitochondrial membrane potential in cultured adult sensory neurons and can reverse deficits in this parameter in STZ-induced diabetic rats supports this notion (T. Huang, N.M.S., A. Verkhratsky, and P.F., unpublished observations). The NT-3 pathway regulating mitochondrial function involves activation of phosphoinositide 3-kinase and downstream regulation of metabolic input into the electron transport chain.

**Interrelation between neurofilament synthesis, transport, and phosphorylation.** Table 3 summarizes the changes in neurofilament biology occurring in the STZ-diabetic rat. Early reductions (i.e., at 1–2 months of STZ-induced diabetes) in axonal transport of neurofilament are most closely correlated with reduced synthesis of transcripts (4–6,44). Between 2 and 3 months of STZ-induced diabetes, the aberrant phosphorylation of neurofilament in the DRG is triggered, which may induce accumulation of NF-H and NF-M and exacerbate the inhibition of neurofilament transport. Alternatively, the increased phosphorylation in DRG is a reflection of a further cessation of neurofilament transport as a consequence of impaired energy reserves (as discussed above), associated with a hypophosphorylation of neurofilament in the proximal axon. In contrast, in the distal axon at a longer time point (6 months) of diabetes, there is an

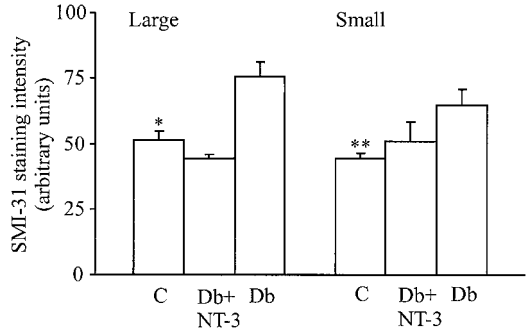


**FIG. 6. NT-3 treatment reduces the levels of NF-H/NF-M phosphorylation in sensory neurons with large somata. Sections of L4 and L5 DRG were analyzed using MetaMorph imaging software to determine the relative levels of fluorescence intensity for each neuron derived using SMI-31 antibody staining (specific for phosphorylated NF-H/NF-M). Large neurons were >30 μm in diameter, and small neurons were <30 μm. Data are expressed in arbitrary units of fluorescence intensity and are means ± SE ($n$ = 36–100 cells for large neurons, $n$ = 17–65 for small neurons). C, control; Db + NT-3, STZ-induced diabetic + NT-3; Db, STZ-induced diabetic. *$P$ < 0.001 for control vs. other groups; **$P$ < 0.001 for control vs. diabetic (one-way ANOVA).**

elevation of neurofilament phosphorylation that is associated with a gross loss of neurofilament and possibly related shrinkage of axon caliber. This increased distal phosphorylation of neurofilament may reflect an attempt to optimize caliber in response to the loss of neurofilament polymers.

**Neuropathological significance of proximal accumulation of neurofilament.** The reduced expression and delivery of neurofilament subunits to the distal axon has been proposed as a critical factor in the etiology of the axonal degeneration observed in diabetic animal models and humans (1,10,11). We propose that the accumulation of NF-H and NF-M in the proximal axon represents a retardation of axonal transport of neurofilament subunits to the distal axon, resulting, in the longer term, in a diminution of distal axon caliber.

NT-3 expression is downregulated in muscle in STZ-diabetic rats (24); therefore, reduced occupancy of trk receptors and $p75^{NTR}$ at nerve endings may contribute to a distally generated stress signal (43) that triggers mitochondrial dysfunction and abnormalities in neurofilament biology (11,24). Although NT-3 treatment corrected the abnormality in neurofilament accumulation, it did not succeed in completely preventing the loss of NF-H and NF-M in sural nerve. The partial 25% increase in NF-M levels in the treated animals may be a reflection of the duration of NT-3 treatment. Two months of treatment may not have been long enough to allow NT-3 to correct the diabetes-induced abnormality causing the accumulation of neurofilament subunits and then, given the slow rate of

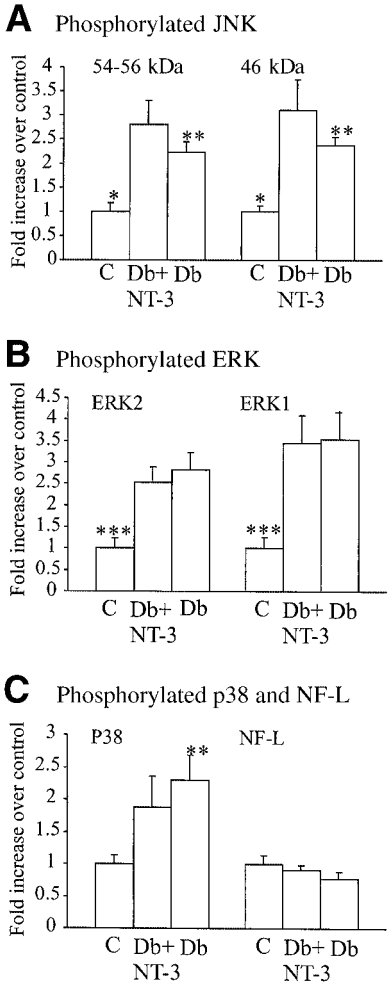


**FIG. 7. NT-3 treatment failed to prevent the activation of SAPKs in DRG of STZ-induced diabetic rats. L4 and L5 DRG were subjected to quantitative western blotting and probed for phosphorylated JNK (54–56kd and 46kd isoforms) (*A*), phosphorylated ERK (ERK1 and ERK2 isoforms) (*B*), and phosphorylated p38 and total NF-L (*C*). Data are normalized to control and are means ± SE ($n$ = 6–9). C, control; Db + NT-3, STZ-induced diabetic + NT-3; Db, STZ-induced diabetic. *$P$ < 0.01 for control vs. diabetic + NT-3 (one-way ANOVA); **$P$ < 0.02 for diabetic vs. control ($t$ test); ***$P$ < 0.05 for control vs. other groups (one-way ANOVA).**

neurofilament axonal transport, permit the transport of the released subunits to the distal axon.

**Conclusion.** The present study showed that the impairment in axonal transport and delivery of neurofilament in sensory neurons in an animal model of type 1 diabetes involves an accumulation of subunits in the proximal area of the peripheral sensory neuraxis. The etiology of this defect may involve loss of neurotrophic support, as NT-3

TABLE 3
Progression of alterations in neurofilament biology in peripheral nerve of experimentally diabetic rats

| Neurofilament expression | 1.5–2 months STZ diabetes | 3 months STZ diabetes | 6–7 months STZ diabetes |
|---|---|---|---|
| NF transcripts in DRG | NF-L, NF-H : ↓ 35–65%* | NF-L, NF-M, NF-H : ↓ 50%† | NF-L, NF-M, NF-H : ↓ 26–46%‡ |
| NF phosphorylation | No change§ | ↑ DRG§,‖; ↓ proximal nerve‖ | ↑ sural nerve§ |
| NF protein/polymers | No change in DRG† | ↑ NFM, NFH protein in DRG and proximal nerve‖<br>↓ NFM, NFH protein in sural nerve‖ | ↓ NF polymer number‡,¶ |

*Mohiuddin et al. (4); †A. Gallagher and P.F., unpublished observations; ‡Scott et al. (1); §Fernyhough et al. (10), and sural nerve data from BB rats (10); ‖present study; ¶Yagihashi et al. (2).

treatment successfully overcame this proximal build-up of protein. Accumulation of neurofilaments may have an impact on the slow anterograde axonal transport of other proteins and explain a range of deficits in diabetes (45). We propose that the outcome of a proximal accumulation of these critical cytoskeletal proteins will, in the longer term, induce detrimental effects on NF-L expression and axonal transport, leading to a failure to maintain the distal axon. These abnormalities in neurofilament biology could explain the distal axonal atrophy seen in experimental and possibly human diabetic neuropathy.

**ACKNOWLEDGMENT**

This work was funded by the Juvenile Diabetes Research Foundation (to P.F.) and National Institutes of Health Grants NS/DK 38855 and DK57629 (to N.A.C.).

**REFERENCES**

1. Scott JN, Clark AW, Zochodne DW: Neurofilament and tubulin gene expression in progressive experimental diabetes: failure of synthesis and export by sensory neurons. *Brain* 122:2109–2117, 1999
2. Yagihashi S, Kamijo M, Watanabe K: Reduced myelinated fiber size correlates with loss of axonal neurofilaments in peripheral nerve of chronically streptozotocin diabetic rats. *Am J Pathol* 136:1365–1373, 1990
3. Mizisin AP, Calcutt NA, Tomlinson DR, Gallagher A, Fernyhough P: Neurotrophin-3 reverses nerve conduction velocity deficits in streptozotocin-diabetic rats. *J Peripher Nerv Syst* 4:211–221, 1999
4. Mohiuddin L, Fernyhough P, Tomlinson DR: Reduced levels of mRNA encoding endoskeletal and growth-associated proteins in sensory ganglia in experimental diabetes mellitus. *Diabetes* 44:25–30, 1995
5. Liuzzi FJ, Bufton SM, Vinik AI: Streptozotocin-induced diabetes mellitus causes changes in primary sensory neuronal cytoskeletal mRNA levels that mimic those caused by axotomy. *Exp Neurol* 154:381–388, 1998
6. Macioce P, Filliatreau G, Figliomeni B, Hassig R, Thiéry J, Di Giamberardino L: Slow axonal transport impairment of cytoskeletal proteins in streptozocin-induced diabetic neuropathy. *J Neurochem* 53:1261–1267, 1989
7. Medori R, Autilio-Gambetti L, Jenich H, Gambetti P: Changes in axon size and slow axonal transport are related in experimental diabetic neuropathy. *Neurology* 38:597–601, 1988
8. Pekiner C, McLean WG: Neurofilament protein phosphorylation in spinal cord of experimentally diabetic rats. *J Neurochem* 56:1362–1367, 1991
9. Terada M, Yasuda H, Kikkawa R: Delayed Wallerian degeneration and increased neurofilament phosphorylation in sciatic nerves of rats with streptozocin-induced diabetes. *J Neurol Sci* 155:23–30, 1998
10. Fernyhough P, Gallagher A, Averill SA, Priestley JV, Hounsom L, Patel J, Tomlinson DR: Aberrant neurofilament phosphorylation in sensory neurons of rats with diabetic neuropathy. *Diabetes* 48:881–889, 1999
11. Fernyhough P, Schmidt RE: Neurofilaments in diabetic neuropathy. *Int Rev Neurobiol* 50:115–144, 2002
12. Julien J-P, Mushynski WE: Neurofilaments in health and disease. *Prog Nucleic Acid Res Mol Biol* 61:1–23, 1998
13. Purves T, Middlemas A, Agthong S, Jude EB, Boulton, AJM, Fernyhough P, Tomlinson DR: A role for mitogen-activated protein kinases in the aetiology of diabetic neuropathy. *FASEB J* 15:2508–2514, 2001
14. Gold BG, Mobley WC, Matheson SF: Regulation of axonal caliber, neurofilament content, and nuclear localization in mature sensory neurons by nerve growth factor. *J Neurosci* 11:943–955, 1991
15. Verge VMK, Tetzlaff W, Bisby MA, Richardson PM: Influence of nerve growth factor on neurofilament gene expression in mature primary sensory neurons. *J Neurosci* 10:2018–2025, 1990
16. Munson JB, Shelton DL, McMahon SB: Adult mammalian sensory and motor neurons: roles of endogenous neurotrophins and rescue by exogenous neurotrophins after axotomy. *J Neurosci* 17:470–476, 1997
17. Ohara S, Tantuwaya V, DiStefano PS, Schmidt RE: Exogenous NT-3 mitigates the transganglionic neuropeptide Y response to sciatic nerve injury. *Brain Res* 699:143–148, 1995
18. Groves MJ, An SF, Giometto B, Scaravilli F: Inhibition of sensory neuron apoptosis and prevention of loss by NT-3 administration following axotomy. *Exp Neurol* 155:284–294, 1999
19. Sterne GD, Brown RA, Green CJ, Terenghi G: Neurotrophin-3 delivered locally via fibronectin mats enhances peripheral nerve regeneration. *Eur J Neurosci* 9:1388–1396, 1997
20. Gao W-Q, Dybdal N, Shinsky N, Murnane A, Schmelzer C, Siegel M, Keller G, Hefti F, Phillips HS, Winslow JW: Neurotrophin-3 reverses experimental cisplatin-induced peripheral sensory neuropathy. *Ann Neurol* 38:30–37, 1995
21. Helgren ME, Cliffer KD, Torrento K, Cavnor C, Curtis R, DiStefano PS, Wiegand SJ, Lindsay RM: Neurotrophin-3 administration attenuates deficits of pyridoxine-induced large-fiber sensory neuropathy. *J Neurosci* 17:372–382, 1997
22. Fernyhough P, Diemel LT, Tomlinson DR: Target tissue production and axonal transport of neurotrophin-3 are reduced in streptozocin-diabetic rats. *Diabetologia* 41:300–306, 1998
23. Ihara C, Shimatsu A, Mizuta H, Murabe H, Nakamura Y, Nakao K: Decreased neurotrophin-3 expression in skeletal muscles of streptozotocin-induced diabetic rats. *Neuropeptides* 30:309–312, 1996
24. Fernyhough P, Tomlinson DR: The therapeutic potential of neurotrophins for the treatment of diabetic neuropathy. *Diabetes Reviews* 7:300–311, 1999
25. Mizisin AP, Kalichman MW, Bache M, Dines KC, DiStefano PS: NT-3 attenuates functional and structural disorders in sensory nerves of galactose-fed rats. *J Neuropathol Exp Neurol* 57:803–813, 1998
26. Patel J, Tomlinson DR: Nerve conduction impairment in experimental diabetes: proximodistal gradient of severity. *Muscle Nerve* 22:1403–1411, 1999
27. Price RL, Paggi P, Lasek RJ, Katz MJ: Neurofilaments are spaced randomly in the radial dimension of axons. *J Neurocytol* 17:55–62, 1988
28. Julien J-P: Neurofilament functions in health and disease. *Curr Opin Neurobiol* 9:554–560, 1999
29. Hirokawa N, Takeda S: Gene targeting studies begin to reveal the function of neurofilament proteins [comment]. *J Cell Biol* 143:1–4, 1998
30. Rao MV, Garcia ML, Miyazaki Y, Gotow T, Yuan A, Mattina S, Ward CM, Calcutt NA, Uchiyama Y, Nixon RA, Cleveland DW: Gene replacement in mice reveals that the heavily phosphorylated tail of neurofilament heavy subunit does not affect axonal caliber or the transit of cargoes in slow axonal transport. *J Cell Biol* 158:681–693, 2002
31. Elder GA, Friedrich VL Jr, Bosco P, Kang CH, Gourov A, Tu PH, Lee VMY, Lazzarini RA: Absence of the mid-sized neurofilament subunit decreases axonal calibers, levels of light neurofilament (NF-L), and neurofilament content. *J Cell Biol* 141:727–739, 1998
32. Jacomy H, Zhu Q, Couillard-Després S, Beaulieu J-M, Julien J-P: Disruption of type IV intermediate filament network in mice lacking the neurofilament medium and heavy subunits. *J Neurochem* 73:972–984, 1999
33. Zhu Q, Couillard-Després S, Julien JP: Delayed maturation of regenerating myelinated axons in mice lacking neurofilaments. *Exp Neurol* 148:299–316, 1997
34. Jung C, Yabe JT, Lee S, Shea TB: Hypophosphorylated neurofilament subunits undergo axonal transport more rapidly than more extensively phosphorylated subunits in situ. *Cell Motil Cytoskeleton* 47:120–129, 2000
35. Nixon RA, Paskevich PA, Sihag RK, Thayer CY: Phosphorylation on carboxyl terminus domains of neurofilament proteins in retinal ganglion cell neurons in vivo: influences on regional neurofilament accumulation, interneurofilament spacing, and axon caliber. *J Cell Biol* 126:1031–1046, 1994
36. Yabe JT, Jung C, Chan WKH, Shea TB: Phospho-dependent association of neurofilament proteins with kinesin in situ. *Cell Motil Cytoskeleton* 45:249–262, 2000
37. Xia CH, Roberts EA, Her LS, Liu X, Williams DS, Cleveland DW, Goldstein LS: Abnormal neurofilament transport caused by targeted disruption of neuronal kinesin heavy chain KIF5A. *J Cell Biol* 161:55–66, 2003
38. Nishikawa T, Edelstein D, Du XL, Yamagishi S, Matsumura T, Kaneda Y, Yorek MA, Beebe D, Oates PJ, Hammes HP, Giardino I, Brownlee M: Normalizing mitochondrial superoxide production blocks three pathways of hyperglycaemic damage. *Nature* 404:787–790, 2000
39. Srinivasan S, Stevens M, Wiley JW: Diabetic peripheral neuropathy: evidence for apoptosis and associated mitochondrial dysfunction. *Diabetes* 49:1932–1938, 2000
40. Obrosova IG, Van Huysen C, Fathallah L, Cao XH, Greene DA, Stevens MJ: An aldose reductase inhibitor reverses early diabetes-induced changes in peripheral nerve function, metabolism, and antioxidative defense. *FASEB J* 16:123–125, 2002
41. Belliveau DJ, Krivko I, Kohn J, Lachance C, Pozniak C, Rusakov D, Kaplan D, Miller FD: NGF and neurotrophin-3 both activate TrkA on sympathetic neurons but differentially regulate survival and neuritogenesis. *J Cell Biol* 136:375–388, 1997
42. Dechant G, Tsoulfas P, Parada LF, Barde YA: The neurotrophin receptor

p75 binds neurotrophin-3 on sympathetic neurons with high affinity and specificity. *J Neurosci* 17:5281–5287, 1997
43. Middlemas A, Delcroix, J-D, Sayers NM, Tomlinson DR, Fernyhough P: Enhanced activation of axonally transported stress-activated protein kinases in peripheral nerve in diabetic neuropathy is prevented by neurotrophin-3. *Brain* 126:1671–1682, 2003
44. Medori R, Jenich H, Autilio-Gambetti L, Gambetti P: Experimental diabetic neuropathy: similar changes of slow axonal transport and axonal size in different animal models. *J Neurosci* 8:1814–1821, 1988
45. Tomlinson DR, Mayer JH: Defects of axonal transport in diabetes mellitus: a possible contribution to the aetiology of diabetic neuropathy. *J Auton Pharmacol* 4:59–72, 1984